European Journal of Neuroscience, Vol. 25, pp. 683–694, 2007 doi:10.1111/j.1460-9568.2007.05317.x

Neuronal death in *Drosophila* triggered by GAL4 accumulation

Carolina Rezával, Santiago Werbajh and María Fernanda Ceriani
Laboratorio de Genética del Comportamiento, Fundación Instituto Leloir, Av. Patricias Argentinas 435, Buenos Aires 1405, Argentina

Keywords: apoptosis, neurodegenerative diseases, protein aggregation

Abstract

The GAL4/UAS system has been extensively employed in *Drosophila* to control gene expression in defined spatial patterns. More recently this system has been successfully applied to express genes involved in neurodegeneration to model various diseases in the fruit fly. We used transgenic lines expressing different levels of GAL4 in a particular subset of neurons involved in the control of rhythmic behaviour, so that its impact on neuronal physiology would result in altered locomotor activity, which could be readily assessed. We observed a striking correlation between *gal4* dosage and behavioural defects associated with apoptotic neuronal loss in the specific GAL4-expressing neurons. Increased *gal4* dosage correlated with accumulation of insoluble GAL4, suggesting that the cascade of events leading to apoptosis might be triggered by protein deposits of either GAL4 or protein intermediates. Behavioural defects were rescued by expression of *hsp70*, a classic chaperone that also interferes with cell death pathways. In agreement with the latter, the viral caspase inhibitor *p35* also rescued GAL4-induced behavioural defects. Our observations demonstrate the intrinsic effects of GAL4 deregulation on neuronal viability and suggest that an excess of GAL4 might enhance neuronal deficits observed in models of neurodegeneration.

Introduction

A striking feature of neurodegenerative diseases is the apparent lack of similarity between the proteins ultimately causing the disease (Ross & Poirier, 2004). The most conspicuous molecular event common among neurodegenerative diseases is the accumulation of abnormal protein aggregates. Some of them show characteristic protein depositions [such as Parkinson's, Alzheimer's and Huntington's diseases (HD)], but in others the correlation between the presence of inclusions and neurodegeneration is less evident (Bird *et al*., 1999; Wittmann *et al*., 2001). More importantly, there is not a clear correlation between the severity of the disease and the degree of aggregated deposits (Arrasate *et al*., 2004; Ross & Poirier, 2005). These observations have led to the concept of disease being triggered by intermediates in protein folding as opposed to the deposition of the inclusion bodies *per se* (Muchowski & Wacker, 2005).

Recently, *Drosophila* has received attention as a model system for studying a group of so-called conformational disorders (Driscoll & Gerstbrein, 2003; Bilen & Bonini, 2005), in particular polyglutamine diseases (Fernandez-Funez *et al*., 2000; Jackson *et al*., 1998; Warrick *et al*., 1998), Parkinson's disease (Feany & Bender, 2000) and tauopathies reminiscent of Alzheimer's disease (Wittmann *et al*., 2001). Surprisingly, *Drosophila* expressing the human or fly homologs of disease genes share a number of the characteristics often described in patients with the disease (Feany & Bender, 2000; Bonini & Fortini, 2003). Likewise, pioneer work has helped establish a correlation between neuronal dysfunction leading to observable behavioural phenotypes and neurodegeneration (Palladino *et al*., 2002; Palladino *et al*., 2003).

Drosophila has also been instrumental in dissecting the molecular basis of rhythmic behaviour (Stanewsky, 2003). Flies display crepuscular behaviour, that is, increased locomotor activity near dawn and dusk but quiescence the rest of the time under light–dark cycles. Under constant conditions this behaviour remains rhythmic with a period of $\sim$24 h. This rhythmicity under free-running conditions depends largely on an intact molecular oscillator (reviewed in Hardin, 2005) and an intact circadian circuitry (Helfrich-Forster, 2003), and is coordinated by the activity of a group of neurons known as the small ventral lateral neurons (LNvs; Helfrich-Forster, 1998; Park *et al*., 2000; Lin *et al*., 2004; Stoleru *et al*., 2005). The small LNvs release a neuropeptide called pigment-dispersing factor (PDF) at the dorsal protocerebrum (Park *et al*., 2000). Interestingly, ablation of the LNvs by overexpression of pro-apoptotic genes causes behavioural arrhythmicity upon transfer to constant darkness (Renn *et al*., 1999).

Employing a transgenic line that expresses GAL4 under the control of the *pdf* promoter region (Renn *et al*., 1999; Park *et al*., 2000) we observed a marked reduction in rhythmicity when *pdf-gal4* was analysed in a homozygous state. The extensive application of the *pdf-gal4* driver line prompted us to investigate the cause underlying this abnormal behaviour. We found that an increased *gal4* gene dose positively correlated with a decrease in behavioural rhythmicity, which in turn was associated with a reduction in the number of small LNvs. Overexpression of HSP70 and baculovirus p35 rescued the arrhythmic phenotype, strongly suggesting that the LNvs were undergoing cell death. Confocal analysis of PDF neurons showed PDF colocalization with TUNEL staining (a marker of nuclear fragmentation), clearly

Correspondence: Dr M. Fernanda Ceriani, as above.
E-mail: fceriani@leloir.org.ar

Received 11 May 2006, revised 19 November 2006, accepted 27 November 2006

indicating that accumulated GAL4 protein triggers cell death via apoptosis. Programmed cell death as a result of over-expression of *gal4* is not a result of a special sensitivity of this neuronal circuit, as similar results were obtained in parallel following continuous GAL4 expression in the developing eye. Moreover, increased GAL4 dosage resulted in its partition to the insoluble fraction, suggesting that even the excess of a protein lacking an endogenous function could lead to neuronal death regardless of a loss of functional phenotype.

Materials and methods

Strains and fly rearing

y w flies were employed as wild-type controls. The following fly lines were provided by the Bloomington Stock Center: *y*[1] *w*[1], P{w[+mC]=Pdf-GAL4.P2.4}X *y*[1] *w*[*], w[*]; P{w[+mC]=GAL4-ninaE.GMR}12, w[*]; P{w[+mW.hs]=FRT(w[hs])}G13 P{w[+mC]=tubP-GAL80}LL2, w[*]; P{w[+mC]=UAS-p35.H}BH1. *y*[1] *w*[*]; P{w[+mC] = *pdf-gal4*.P2.4} was kindly provided by Jeff Hall (Brandeis University), UAS-HSPA1L/Cyo by Nancy Bonini (University of Pennsylvania) and UAS-GFP-*lacZ* (II), originally generated by Shigeo Hayashi (Riken Center for Developmental Biology), by P. Wappner (Fundación Instituto Leloir).

Drosophila cultures were maintained on a 12–12 h light–dark cycle on standard corn meal yeast agar medium at 25 °C in an environmental chamber.

Behavioural analyses

Locomotor behaviour was evaluated in young (0- to 3-day-old) males. Fly activity was monitored under light–dark cycles for 4 days when flies were released into constant darkness for at least 1 week, employing commercially available activity monitors (TriKinetics, Waltham, MA, USA). Activity of individual young males throughout the period analysed was displayed on individual actograms. Period and rhythmicity were estimated using the ClockLab software (Actimetrics, Evanston, IL, USA), restricted to data obtained in constant darkness. Flies with a single peak over the significance line in a χ^2 analysis were scored as rhythmic ($P < 0.05$); this was confirmed by visual inspection of the actograms. Flies classified as weakly rhythmic (Ceriani *et al*., 2002) were not taken into account for average period calculations.

Behavioural analyses were performed employing males exclusively, whereas all the remaining experiments included female and male flies of age and sex matched to controls.

Immunohistochemistry and imaging

Brains were dissected at zeitgeber time (ZT)2; (ZT0 indicates the time when the lights were switched on) from 3- to 5-day-old flies pinned down to a Sylgard dish in phosphate-buffered saline (PBS). Brains were fixed in 4% paraformaldehyde in PB (KH_2PO_4, 100 mM; Na_2HPO_4, 100 mM) for 30 min−1 h at room temperature, and then rinsed three times in PT (PBS with 0.1% Triton X-100). Brains were then blocked in 5% goat serum in PT for 2 h at room temperature. After the blocking step, tissue was incubated with the primary antibody for 72 h at 4 °C and then washed three times with PT for 20 min, followed by incubation with the secondary antibody. After staining, brains were washed three times with PT and mounted in 80% glycerol (in PT).

The primary antibody used was rabbit anti-PDF (1 : 5000; from F. Rouyer, CNRS, France). The secondary antibodies used were Cy3-conjugated donkey anti-rabbit and Alexa 594 (1 : 250; Jackson ImmunoResearch).

Microscopy

The small LNvs of larval brains were visualized directly (without fixation and immunolabelling) in a BX-60 Olympus microscope (equipped with fluorescence, Nomarski optics and dark-field) and photographed with a CoolSnap Pro digital camera. Alternatively, a Zeiss LSM510 confocal microscope was used to image large and small LNvs on whole adult brains.

Fly eyes were imaged on an environmental scanning electron microscope (ESEM) at room temperature. The frontal head semithin sections (1 μm) were performed on fixed tissue (3% glutaraldehyde in PBS for 2 h at room temperature), stained for 1–2 h in 1% osmium tetroxide, dehydrated through ethanol steps and embedded in Spurr's epoxy resin.

TUNEL assay

Young adult (3- to 5-day-old) brains were dissected in PBS and fixed in 4% paraformaldehyde in PBS for 30 min at room temperature. Tissue was washed twice in 0.3% Triton X-100 in PBS (PBST) for 5 min each time, blocked with 5% normal goat antiserum in PBST for 15 min at room temperature and first washed in PBST and then washed in PBS (5 min each time). TUNEL staining was performed using the apoptag plus fluorescein *in situ* apoptosis detection kit (S7111; Amersham Biotech) following manufacturer's instructions. Brains were mounted in 80% glycerol in PBS and visualized in a Zeiss LSM510 confocal microscope.

Statistical analysis

Data obtained in Figs 1 and 4 were analysed employing ANOVA followed by pairwise comparisons employing Student's *t*-test with the Bonferroni correction. Data from Figs 2 and 5 were analysed using a χ^2 test. The *P*-values are indicated in the corresponding figure legends.

Protein solubility assay

This procedure was based on the protocols described by Lee and colleagues and Bonini and collaborators (Skovronsky *et al*., 1998; Auluck *et al*., 2005) with modifications, as follows.

Sixty fly heads of the appropriate age (0–3 days and 20 days old) were frozen on dry ice and then homogenized in RIPA buffer [deoxycholate, 0.5%; SDS, 0.1%; NP40, 1%; and EDTA, 5 mM; in PBS 1× with a cocktail of general protease inhibitors (Sigma)] and incubated on ice for 30 min. Soluble and insoluble fractions were separated by ultracentrifugation at 100 000 ***g*** at 4 °C for 40 min. The pellets were suspended in 200 μL of 70% formic acid with sonication until clear, and then ultracentrifuged at 100 000 ***g*** at 4 °C for 40 min. The formic acid was removed by vacuum centrifugation for 4 h, and the resulting pellet was resuspended in 60% acetonitrile. RIPA buffer (1.9 mL) was added to each sample. Both RIPA-soluble and formic acid-soluble fractions were subjected to immunoprecipitation with 1 μg anti-GAL4 DNA binding domain mouse monoclonal antibody (Santa Cruz Biotechnology) and protein G-agarose (Amersham Biosciences). Immunoprecipitated GAL4 was resolved on an 8% TRIS–Gly polyacrylamide gel. Proteins were transferred to PVDF membrane (Amersham Biosciences) and probed with anti-GAL4 TA

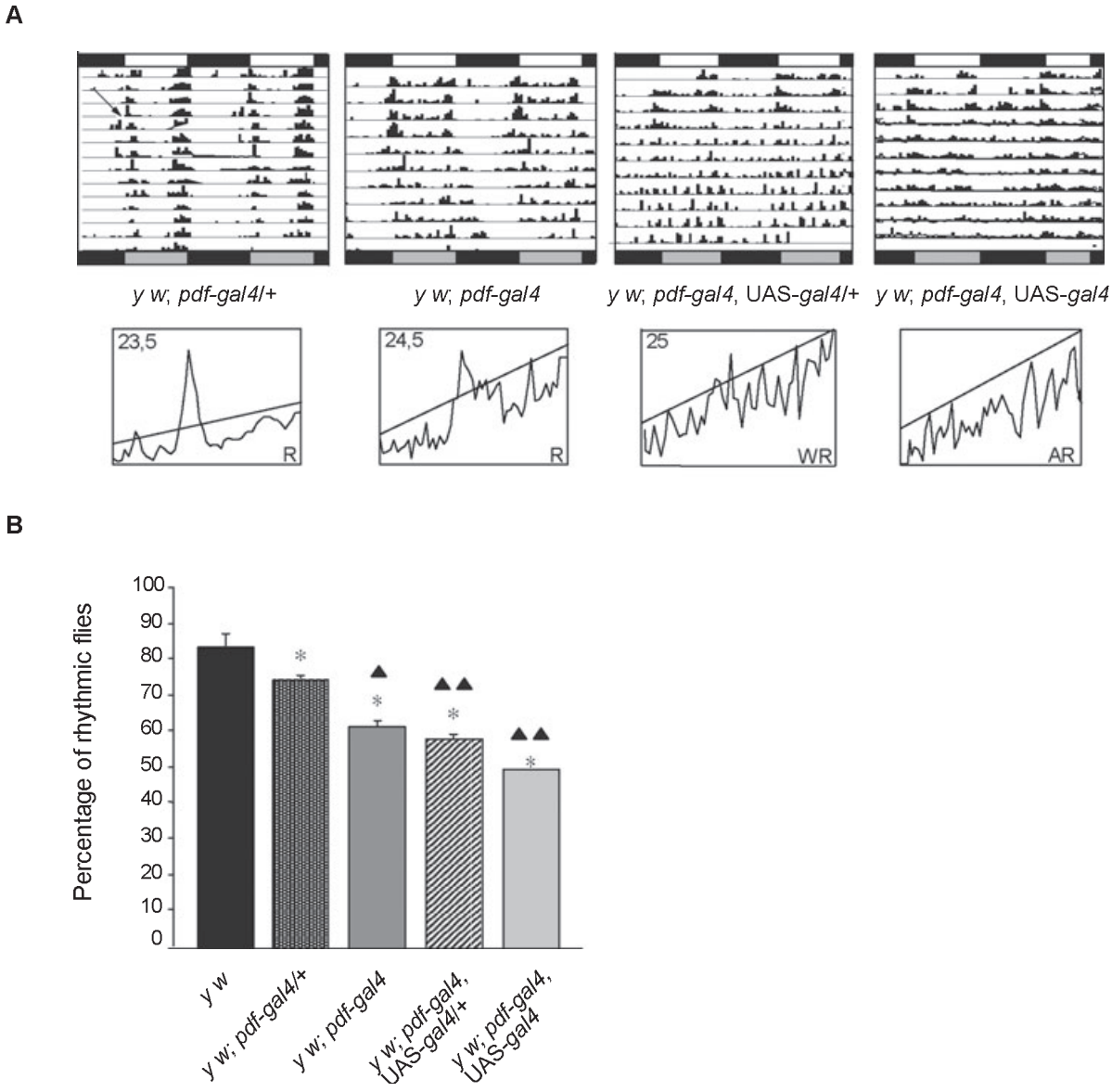

FIG. 1. GAL4 overexpression in lateral neurons caused behavioural arrhythmicity. Fly lines representing different levels of GAL4 were evaluated. The recombinant line *pdf-gal4*,UAS-*gal4* in homozygosis expresses the highest level of GAL4. Locomotor activity was monitored employing an automated setup. Experiments were performed at least three times. (A) Representative double-plotted (each row representing two consecutive days) actograms (top panels) and the corresponding periodograms (bottom panels) are shown: the free-running period is indicated in the upper left corner. The arrow, which applies to all panels, indicates the day of transfer to constant darkness. Open and filled bars indicate day and night phases, respectively, the shaded bars indicating 'day' during the period of constant darkness. R, rhythmic; WR, weakly rhythmic; AR, arrhythmic in the periodogram analysis ($P < 0.05$). (B) Percentage of rhythmic flies for each strain is shown. All flies included in Table 1 were taken into account for this analysis. Statistical analysis included ANOVA and pairwise comparisons employing Student's *t*-test with the Bonferroni correction. All the strains containing at least one copy of *gal4* were significantly different from *y w* (*$P < 0.001$). Genotypes significantly different from *pdf-gal4/+*: ($^{▲}P < 0.01$) *pdf-gal4* and ($^{▲▲}P < 0.001$) *pdf-gal4*,UAS-*gal4/+* and *pdf-gal4*,UAS-*gal4*.

mouse monoclonal antibody (1 : 2000; Santa Cruz Biotechnology) followed by secondary antibody with HRP-conjugated antimouse antibody (1 : 10000; Jackson ImmunoResearch), revealed using ECL+ (Amersham Biosciences) and analysed in a Storm Phosphoimager employing the Image Quant software.

Results

Increasing gal4 *dosage was responsible for disorganising rhythmic locomotor behaviour*

In the context of a genetic screen it was noticed that homozygous lines expressing *gal4* in the LNvs (*pdf-gal4*) were on average less rhythmic than their heterozygous counterparts, which in turn did not show such consolidated behaviour as wild-type flies. To determine whether GAL4 levels could account for this effect a recombinant line containing a copy of *pdf-gal4* and a copy of the upstream activating sequence (UAS) driving *gal4* (UAS-*gal4*) was generated (*pdf-gal4*,UAS-*gal4*). This line should depend on the restricted distribution of the *pdf* promoter to trigger *gal4* expression, but once GAL4 accumulated within the LNvs it should direct *gal4* expression *de novo* by recognition of its target sequence UAS. As a result there should be a substantial amplification of the original GAL4 levels in these cells.

Heterozygous and homozygous flies expressing these constructs were evaluated in an automated locomotor behaviour setup.

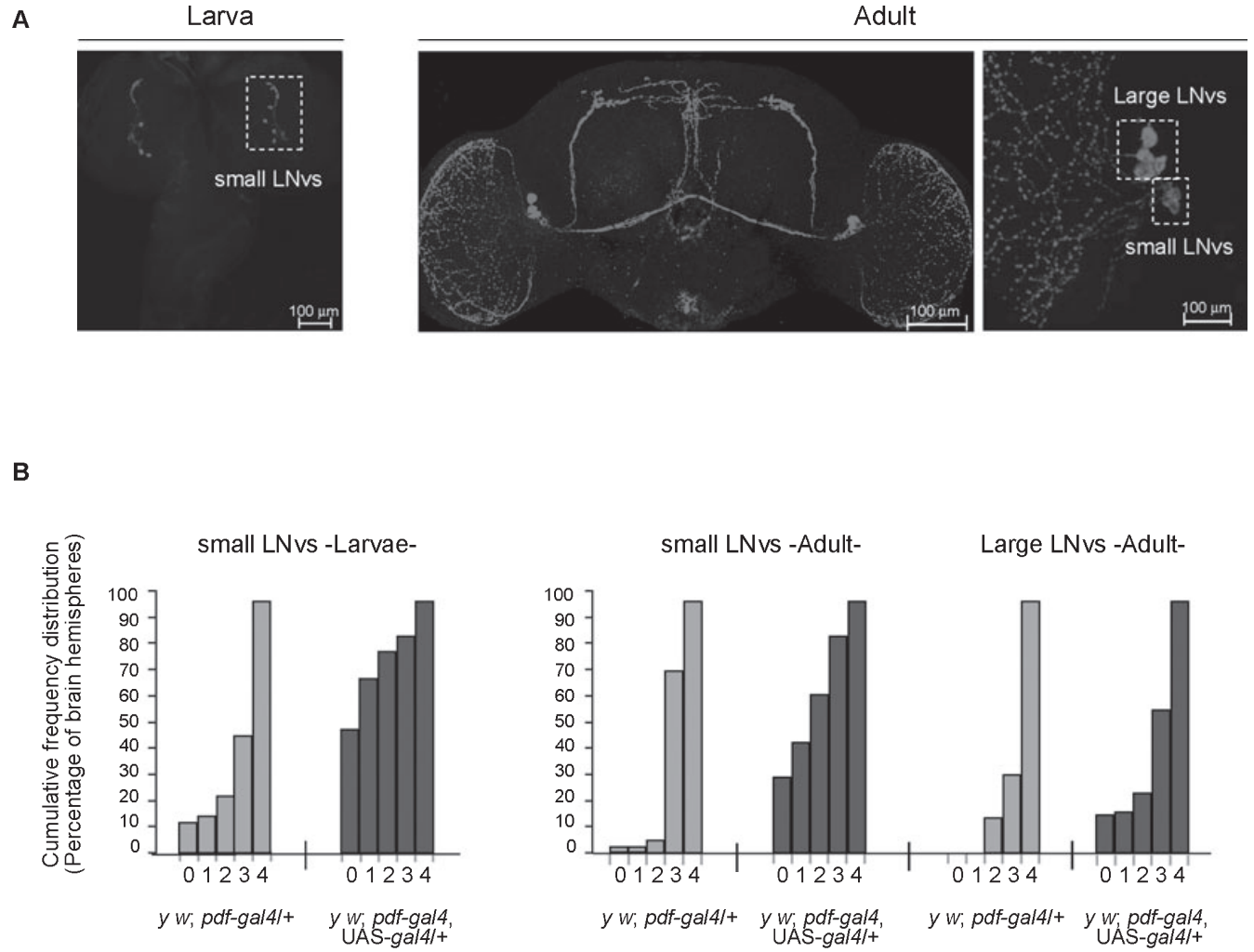

FIG. 2. Alterations in the PDF circuitry were responsible for the behavioural arrhythmicity. (A) Whole-mount brain immunofluorescence of *y w* flies stained for PDF antibody showed the normal four and eight lateral neurons per hemisphere for, respectively, larvae (left panel) and adults (middle and right panels). (B) *pdf-gal4*/UAS-GFP ($n = 52$) and *pdf-gal4*,UAS-*gal4*/UAS-GFP ($n = 61$) larval brains were dissected without fixation and the number of GFP^+ neurons per hemisphere was counted. The number of adult lateral neurons per hemisphere was counted in *pdf-gal4*/+ ($n = 29$) and *pdf-gal4*,UAS-*gal4* ($n = 93$) fly brains stained for PDF. The difference between adult and larval small LNv clusters might reflect the fact that brains not showing any PDF^+ signal in either brain hemisphere (presumably more common at the adult stage) were discarded from the analysis. Tests of independence using χ^2 analysis showed significant differences between the cumulative frequency distribution of lateral neuron numbers in larval ($P < 0.05$) and adult ($P < 0.05$) small LNs per hemisphere. No differences in the distribution in the large LNv cluster were observed.

Heterozygous *pdf-gal4* along with wild-type flies displayed rhythmic activity consolidated around dawn and dusk, and continued to do so for days under constant darkness (Fig. 1A). In contrast, as GAL4 levels increased, rest activity cycles appeared less synchronized under both light–dark and constant dark conditions. Periodogram analysis confirmed these observations as individual flies bearing a combination of the two transgenes became weakly rhythmic (heterozygotes) and eventually arrhythmic (homozygotes). Representative actograms of the increasing *gal4* gene dosage are shown, along with the corresponding periodograms, in Fig. 1A. Figure 1B shows the percentage of rhythmic flies characteristic of each category. Every fly line containing at least one copy of *gal4* was statistically significantly different from wild-type flies from a matched genetic background. Homozygous *pdf-gal4* and the *pdf-gal4*,UAS-*gal4* lines were significantly less rhythmic than the *pdf-gal4* heterozygous line (from now on referred to as the 'control'). Interestingly, the addition of a nonrelated UAS transgene (as in *pdf-gal4*,UAS-*gal4*/UAS-GFP; Table 1) did not alter the GAL4-associated defect on rhythmicity (Table 1), suggesting that this effect cannot be attributed to high GAL4 levels in the absence of its target sequence.

To entertain the possibility of a positional effect due to the *pdf-gal4* insertion on the second chromosome a similar analysis was performed with an X chromosome line. As shown in Table 1, hemizygous *pdf-gal4* males showed a similar decrement in rhythmicity, clearly pointing to a GAL4-dependent defect as opposed to one triggered by the P element insertion.

Loss of rhythmicity was associated with a decreased number of larval precursors and adult neurons

The larval PDF circuit comprises four small lateral neurons per brain hemisphere; they stained positive for this neuropeptide (Fig. 2A). They are clearly seen in third instar larval brains and stay intact through metamorphosis, giving rise to the adult small LNvs. The four

TABLE 1. Free-running rhythmicity behaviour in flies entrained to 12–12 h light–dark cycles for 4 days and then released into constant darkness and monitored for a further 7–10 days

Genotype	*n*	Rhythmicity (% of group)			Mean period (h)	FFT
		R	WR	AR		
y w	32	83.98	13.80	2.22	23.6 ± 0.72	0.10 ± 0.01
y w; *pdf-gal4*/+	66	74.93	25.21	1.00	23.63 ± 0.26	0.10 ± 0.01
y w; *pdf-gal4*	21	61.82	33.64	4.55	24.46 ± 0.31	0.09 ± 0.01
y w; *pdf-gal4*,UAS-*gal4*/+	70	58.35	39.27	2.38	23.85 ± 0.09	0.10 ± 0.01
y w; *pdf-gal4*,UAS-*gal4*	30	50.00	50.00	0.00	23.83 ± 0.12	0.11 ± 0.01
y w; *pdf-gal4*,UAS-*gal4*/*tub-gal80*	31	59.60	34.85	5.56	24.05 ± 0.11	0.13 ± 0.01
y w; *pdf-gal4*,UAS-*gal4*/UAS-*hsp70*	48	81.13	17.49	1.39	23.64 ± 0.07	0.12 ± 0.01
y w; *pdf-gal4*,UAS-*gal4*/UAS-*p35*	60	79.24	20.76	0.00	23.86 ± 0.09	0.14 ± 0.01
y w; *pdf-gal4*,UAS-*gal4*/UAS-GFP	28	57.14	42.86	0.00	23.63 ± 0.06	0.13 ± 0.01
pdf-gal4; ;	14	42.86	57.14	0.00	24.67 ± 0.17	0.07 ± 0.02
y w; *tub-gal80*/+	29	82.76	6.90	10.34	23.44 ± 0.13	0.13 ± 0.01

Locomotor activity: R, rhythmic; WR, weakly rhythmic; AR, arrhythmic ($P < 0.05$). Period values were determined using ClockLab employing χ^2 periodogram analysis, taking into account only rhythmic individuals. The mean power fast Fourier transform (FFT) for these flies is shown (power is a quantification of the strength of the circadian rhythm).

large LNvs, on the other hand, develop during mid-pupal stages (Helfrich-Forster, 1997). Taghert and colleagues originally reported that overexpression of a pro-apoptotic gene under *pdf-gal4* caused arrhythmicity a few days after transfer to constant darkness (Renn *et al*., 1999). To determine whether the lack of rhythmicity observed in our experiments originated from the loss of lateral neurons, whole-brain immunofluorescence was performed on larval and adult *pdf-gal4*,UAS-*gal4* brains. Larval brains were inspected directly for GFP fluorescence; meanwhile, adult brains were immunolabelled with anti-PDF. GFP/PDF$^+$ somas stained with the specific antiserum were counted in each brain hemisphere and the cumulative frequency distribution displaying 0–4 LNvs is shown in Fig. 2B.

The distribution was statistically significantly different between control and recombinant larval brains, indicating that *pdf-gal4*,UAS-*gal4*/UAS-GFP contained on average fewer small LNvs than the *pdf-gal4*/UAS-GFP line. A similar observation was made when adult small LNv clusters were analysed (Fig. 2B).

Introducing a reporter gene under the control of a UAS (UAS-GFP) in both control and *pdf-gal4*,UAS-*gal4* lines led to similar results, confirming that lack of rhythmicity was derived from a reduced number of small LNvs.

On the other hand, when the large LNvs were compared, the *pdf-gal4*,UAS-*gal4* line contained on average fewer PDF$^+$ somas, although the frequency distribution was not statistically significantly different from that of the controls. A possible explanation would be that this cluster switched on *pdf* expression later in development and thus had probably been accumulating GAL4 for a shorter period of time. Alternatively, the susceptibility to GAL4 accumulation could differ between the two LNv clusters.

PDF neurons were undergoing apoptotic cell death

Loss of PDF neurons in the *pdf-gal4*,UAS-*gal4* line opened the possibility that elevated GAL4 levels could be triggering neuronal death. To test this hypothesis, TUNEL staining was performed on *pdf-gal4*,UAS-*gal4* and heterozygous *pdf-gal4* lines. Wild-type brains occasionally showed positive TUNEL staining, although no example was found to colocalize with the small or large LNvs (Fig. 3A, top panel). Conversely, in several independent experiments homozygous *pdf-gal4*,UAS-*gal4* lines retrieved a positive TUNEL staining within the PDF$^+$ cluster. A striking example of such colocalization is shown in Fig. 3A (bottom panel), in which three PDF$^+$ cells in each brain hemisphere were undergoing apoptosis at the time the brain was dissected and fixed. TUNEL staining within the PDF circuit in the *pdf-gal4*,UAS-*gal4* line was also detected in larval brains (data not shown).

We speculated that protein misfolding could somehow be involved in triggering apoptosis. Whole-mount immunofluorescence on young and aged adult brains was performed to search for protein inclusions. Surprisingly, even employing several different commercial antibodies, no GAL4-specific signal could be detected (data not shown), suggesting that either the amount of aggregated protein was limited or the relevant epitopes were hidden within the aggregates. Detection of aggregated proteins was also attempted employing thioflavine-S staining (Greeve *et al*., 2004), but no clear results were obtained either (data not shown), strengthening the possibility of a limited amount of aggregated protein as the most probable explanation for the lack of detection. Along the same lines, GAL4 could not be detected by direct Western blotting of fly-head extracts, probably due to the fact that only eight neurons per brain hemisphere at most were expressing GAL4 in the adult stage. Thus far it was unclear whether cell death was the result of aggregation or not.

To increase the sensitivity of the technique, protein extracts were prepared from young or aged heterozygous and homozygous *pdf-gal4*,UAS-*gal4* flies, and the soluble and insoluble fractions were separated by centrifugation followed by immunoprecipitation and Western blotting (Fig. 3B). In both the heterozygous and homozygous *pdf-gal4*,UAS-*gal4* lines a tendency to accumulate less soluble GAL4 as the flies aged was observed, and this appeared to be more robust in the former. In addition, we noticed that the homozygous *pdf-gal4*,UAS-*gal4* line accumulated less GAL4 in the soluble fraction than a genotype with half the *gal4* dose. These observations suggested that GAL4 was excluded from the soluble fraction and prompted the evaluation of GAL4 accumulation in the insoluble fraction. In agreement with the decrement in the soluble fraction with time, GAL4 was detected in the insoluble fraction in young *pdf-gal4*,UAS-*gal4* flies and increased about four- to five-fold as the flies aged.

Taken together, these results suggest that higher levels of GAL4 might trigger conformation defects leading to partition of the misfolded protein to the insoluble fraction, ultimately leading to apoptosis.

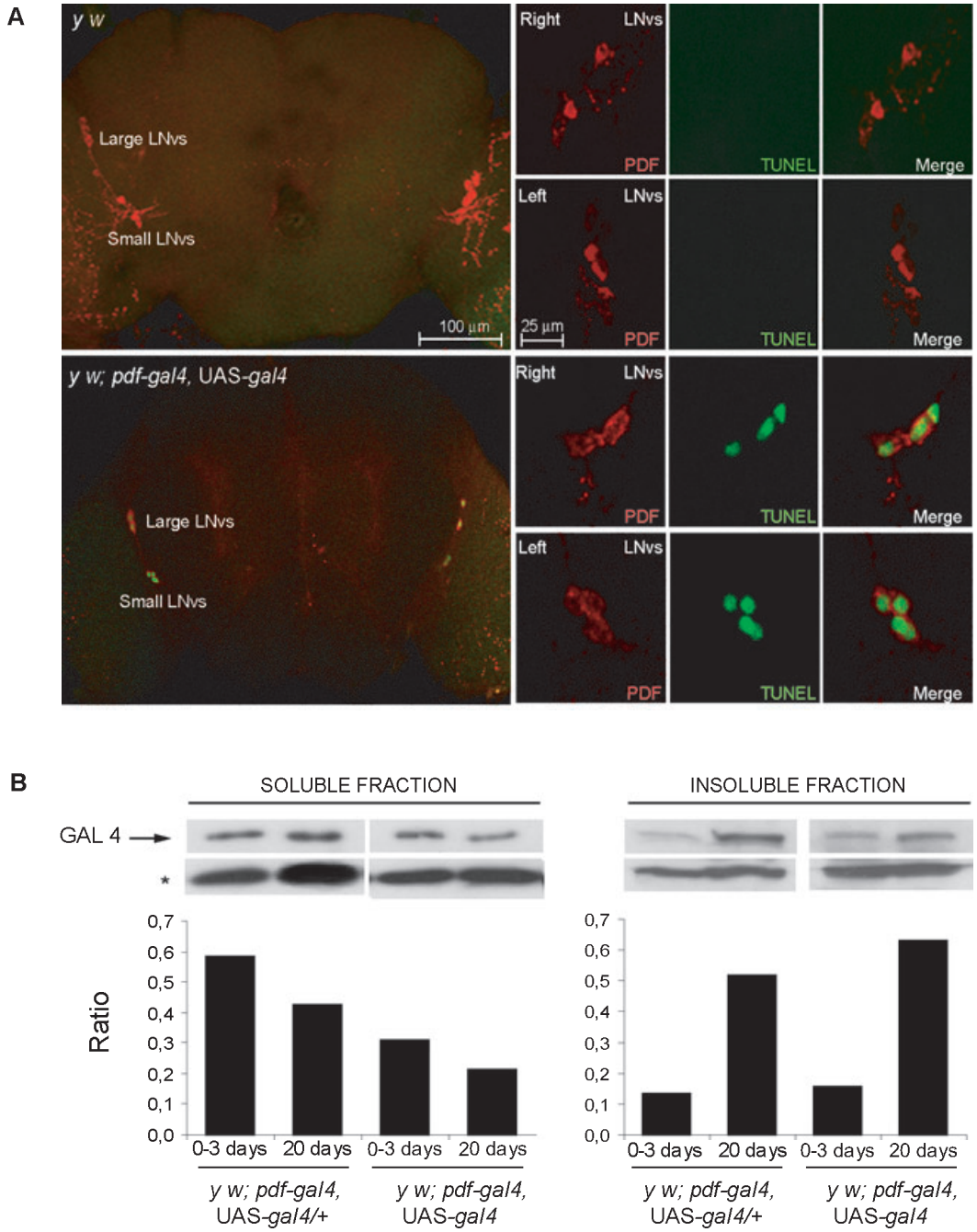

FIG. 3. GAL4 accumulated in the insoluble fraction and triggered cell death through an apoptotic pathway. (A) TUNEL and PDF immunofluorescence was performed on *y w* and *pdf-gal4*,UAS-*gal4* adult brains. Young adult (3- to 5-day-old) brains were dissected and fixed, and the staining was performed using Apoptag *in situ* apoptosis detection. Brains were mounted in 80% glycerol in PBS and visualized via a confocal microscope. Insets show a magnified view of the small LNvs for each genotype. This phenomenon was observed in at least one brain per experiment for *pdf-gal4*,UAS-*gal4* flies ($n = 7$–15) but no example was found to colocalize within the LNvs in wild-type brains ($n = 6$–16). Staining in larvae and adult brains was performed three times with similar results. (B) Western blot of the RIPA-soluble (upper left panel) and formic acid-soluble fraction (upper right panel) for the heterozygote and homozygote genotypes at 0–3 days and 20 days, respectively, immunoprecipitated with a mouse monoclonal antibody directed to the binding domain of GAL4. The antibodies employed in the immunoprecipitation and Western blotting were directed against different portions of the protein. The GAL4-specific (arrow) and a nonspecific (*) band were quantified employing the Image Quant software (Storm Phosphoimager). The ratio between GAL4 and the nonspecific band is shown in the lower panel. Experiments were performed three times with similar results; a representative example is shown.

Blocking programmed cell death was sufficient to rescue behavioural defects

To begin to address the mechanism in time responsible for the loss of PDF neurons, potential modifiers of GAL4 activity were introduced into the *pdf-gal4*,UAS-*gal4* line. Constitutive expression of GAL80, a specific repressor of GAL4 transcriptional activity (Ma & Ptashne, 1987), in the context of the heterozygous *pdf-gal4*,UAS-*gal4* line retrieved ~60% of rhythmic flies (Fig. 4 and Table 1), which was not statistically significantly different from the *pdf-gal4*,UAS-*gal4* line itself, precluding the possibility that the

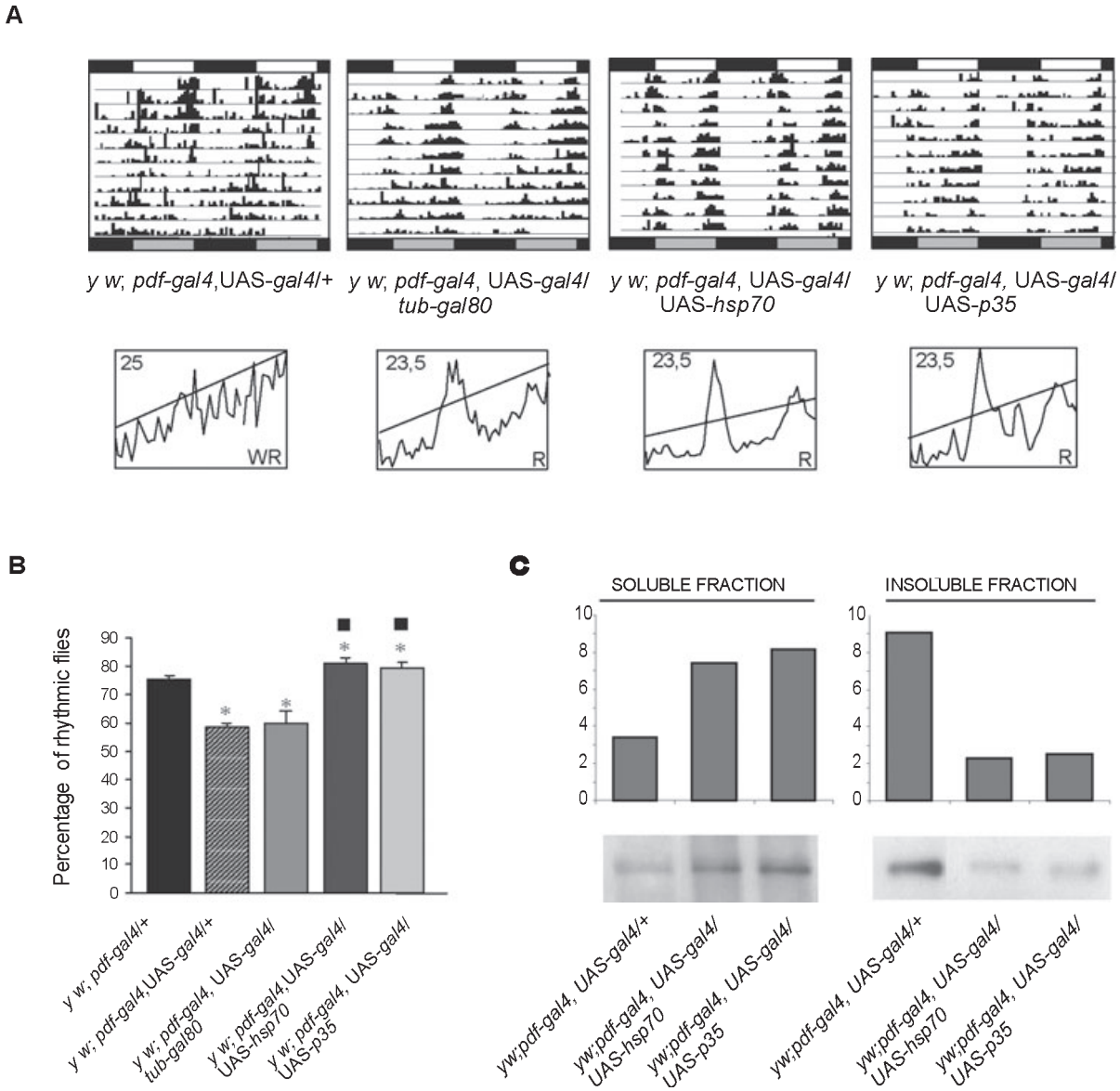

FIG. 4. Overexpression of HSP70 and P35 rescued the locomotor activity defects. Locomotor activity experiments were performed at least three times. (A) Representative double-plotted actograms (top panels) and the corresponding periodograms (bottom panels) for each genotype are shown. Arrows indicate the day of transfer to constant darkness. R, rhythmic; WR, weakly rhythmic; AR, arrhythmic; fuller explanation in legend to Fig. 1. (B) Percentage of rhythmic flies for each strain is shown. All flies included in Table 1 were taken into account for this analysis. Statistical analysis included ANOVA and pairwise comparisons employing Student's *t*-test with the Bonferroni correction. All the strains containing at least a copy of *pdf-gal4*,UAS-*gal4/+* were significantly different from *pdf-gal4/+* (*$P < 0.001$). *pdf-gal4*,UAS-*gal4/*UAS-*hsp*70 and *pdf-gal4*,UAS-*gal4/*UAS-p35 were significantly different from *pdf-gal4*,UAS-*gal4/+* (■$P < 0.001$). (C) Western blot of the RIPA-soluble (left panel) and formic acid-soluble fraction (right panel) for 20-day-old heterozygote *pdf-gal4*,UAS-*gal4* in the context of UAS-*hsp70* and UAS-*p35*. Samples were quantified by Bradford assay prior to immunoprecipitation, and equal amount of extracts were loaded into each lane. The antibodies employed in the immunoprecipitation and Western blotting were directed against different portions of the protein. The GAL4-specific band was quantified employing the Image Quant software (Storm Phosphoimager). Experiments were performed three times with similar results; a representative example is shown.

activation of nonspecific targets could be responsible for the phenotypes observed.

Based on our observations that GAL4 overload correlated with a positive TUNEL staining we introduced a copy of UAS-*p35* into the *pdf-gal4*,UAS-*gal4* line. Baculovirus P35 is a general caspase inhibitor, and has been shown to have an antiapoptotic effect when expressed in the fly eye (Hay *et al*., 1994) and to modulate degeneration in brain models of SCA1 and SCA3 (Ghosh & Feany, 2004). *pdf-gal4*,UAS-*gal4/*UAS-*p35* flies showed a marked increase in the percentage of rhythmic individuals, also significantly different from the *pdf-gal4*,UAS-*gal4* and *pdf-gal4* heterozygous lines, indicating that apoptosis could account for the loss of rhythmicity observed in the former, irrespective of the protein overload (Fig. 4).

Likewise, heat-shock protein 70 (HSP70) has been employed to modulate deleterious effects caused by over-expression of aggregating proteins, among others SCA1, SCA3 and α-SYNUCLEIN (Warrick *et al*., 1999; Chan *et al*., 2000; Auluck *et al*., 2002; Ghosh & Feany, 2004). As a correlation between GAL4 transcriptional activity and loss of rhythmicity could not be unequivocally established, and an excess of GAL4 in time caused this protein to accumulate in the insoluble fraction (Fig. 3B), the effect of HSP70 expression on behavioural performance was explored. Strikingly, introducing a single copy of

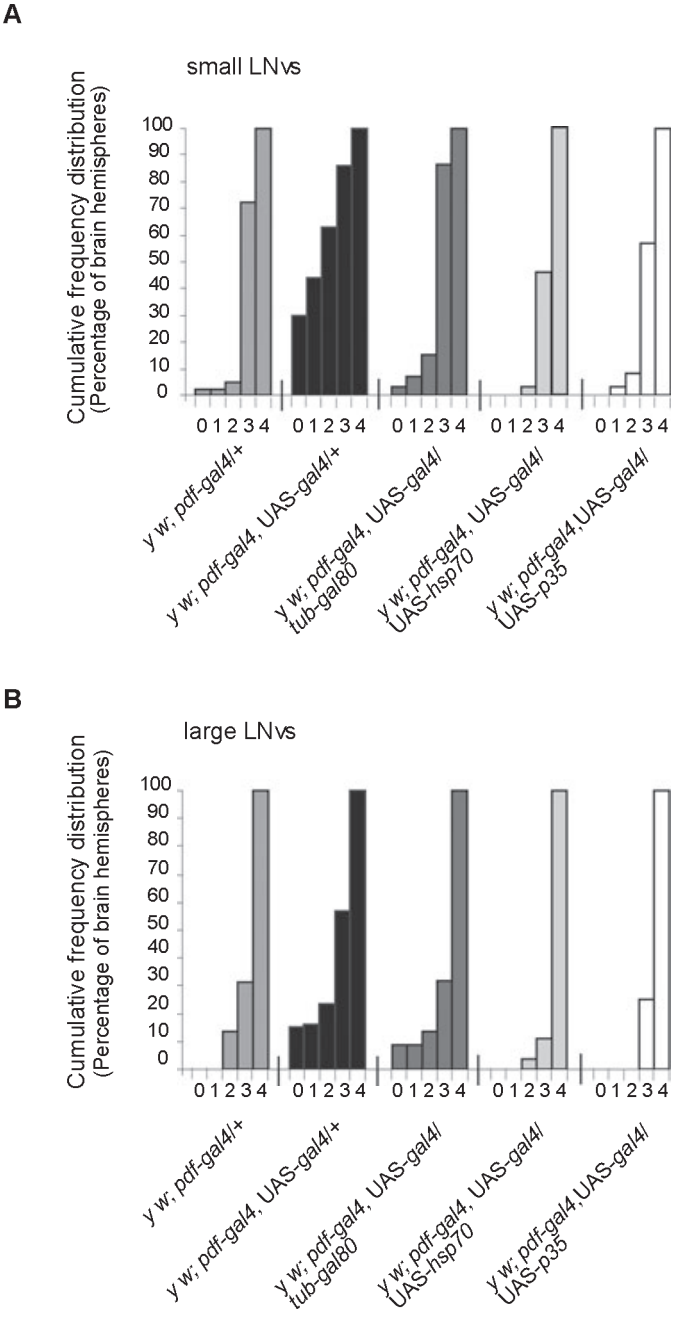

FIG. 5. Overexpression of HSP70 and P35 restored the normal number of lateral neurons. The number of adult lateral neurons per hemisphere stained for PDF was counted in *pdf-gal4*,UAS-*gal4/+* ($n = 90$), *pdf-gal4*,UAS-*gal4/*tub-*gal*80 ($n = 22$), *pdf-gal4*,UAS-*gal4/*UAS-*hsp70* ($n = 27$) and *pdf-gal4*,UAS-*gal4/*UAS-*p35* ($n = 28$). χ^2 Analysis showed significant differences in the cumulative frequency distributions of small LNv numbers per hemisphere (A) when comparing *pdf-gal4*,UAS-*gal4/*UAS-*hsp70* ($P < 0.01$) or *pdf-gal4*,UAS-*gal4/*UAS-*p35* ($P < 0.05$) to *pdf-gal4*,UAS-*gal4/+*. No significant differences were observed in any group in the large LNv cluster (B). Deleterious effects of GAL4 were independent of the cell type.

UAS-*hsp70* into the *pdf-gal4*,UAS-*gal4* line returned rhythmicity to wild-type levels. Moreover, the percentage of rhythmic individuals was significantly different from both the recombinant and wild-type controls (Fig. 4A and B), suggesting a 'beneficial' effect of HSP70 even at the lower end of GAL4 accumulation (Bonini, 2002). HSP70 could prevent toxicity associated with abnormal accumulation of misfolded proteins by virtue of its activity as a molecular chaperone, that is, by guiding proper folding of proteins with a tendency to aggregate. Alternatively, as has recently been shown, HSP70 could modulate the apoptotic pathway in a more direct fashion (Saleh *et al*., 2000; Yenari *et al*., 2005).

To begin to address this possibility, protein extracts were prepared from aged heterozygous *pdf-gal4*,UAS-*gal4* flies in the context of modulators of GAL4 activity, and the soluble and insoluble fractions were separated by centrifugation followed by immunoprecipitation and Western blotting (Fig. 4C). Expression of both HSP70 and P35 resulted in increased soluble GAL4. This phenomenon was accompanied by a marked reduction in GAL4 levels in the insoluble fraction, down to roughly one-third of the amount observed in *pdf-gal4*,UAS-*gal4* flies. Changes in protein solubility by coexpression of regulators of cell death are not unprecedented. In this regard, Sang *et al*. (2005) reported that reducing APAF-1 activity modulated protein aggregation and cell death in an HD model. This observation would favour the hypothesis that insoluble GAL4 is associated with decreased rhythmicity.

Effective modulators of GAL4 effects were associated with a functional PDF circuit

To confirm whether over-expression of GAL4 modulators restored rhythmicity by preventing neuronal loss, as opposed to simply improving the physiological state of the remaining neurons, we performed whole-mount immunofluorescence on adult brains. A cumulative frequency distribution for each independent cluster is shown in Fig. 5. In the heterozygous *pdf-gal4*,UAS-*gal4* line a higher proportion of brains exhibited fewer small LNv neurons, of which $\sim 60\%$ contained only two or fewer, in contrast to $\sim 5\%$ in the control (*pdf-gal4/+*). Phenotype rescue by expression of different modulators of this GAL4-associated defect indicated that HSP70 most efficiently reversed the detrimental effects linked to elevated GAL4 levels, resulting in only 5% of the brains containing fewer than two neurons (same as in the control). In accordance with the reported locomotor activity experiments, expression of GAL80 prevented cell death less efficiently than that of HSP70 or P35, where $\sim 80\%$ of the dissected brains showed fewer than three neurons. The small LNv cluster showed stronger signs of the deleterious GAL4 effects, probably due to the earlier onset of *gal4* expression (first instar larvae: Malpel *et al*., 2002) as opposed to the large cluster, which only develops during mid-metamorphosis (Helfrich-Forster, 1997). In any event, the same trend was observed when expressing the different modulators of GAL4 activity in this cluster, that is, HSP70 and P35 most effectively rescued the deleterious effects associated with GAL4 accumulation (see Figs 4 and 5 for comparison).

GAL4 accumulation affected cell viability in different structures

To examine whether the effect of GAL4 on the PDF circuit resulted from a special sensitivity of this neuronal cluster we expressed GAL4 throughout eye development under the promoter of the *glass* gene (GMR-*gal4*). The adult compound eye presents a regular hexagonal array of ~ 750 facets or ommatidia (Ready *et al*., 1976), which can be observed in detail employing an ESEM (as in Fig. 6). Internally, an ommatidium is a precise 19-cell assembly of eight photoreceptors and 11 accessory cells (the so-called pigment and cone cells), readily identifiable in histological sections; sections taken at different depths within the structure allow the observation of a different number and group of cells.

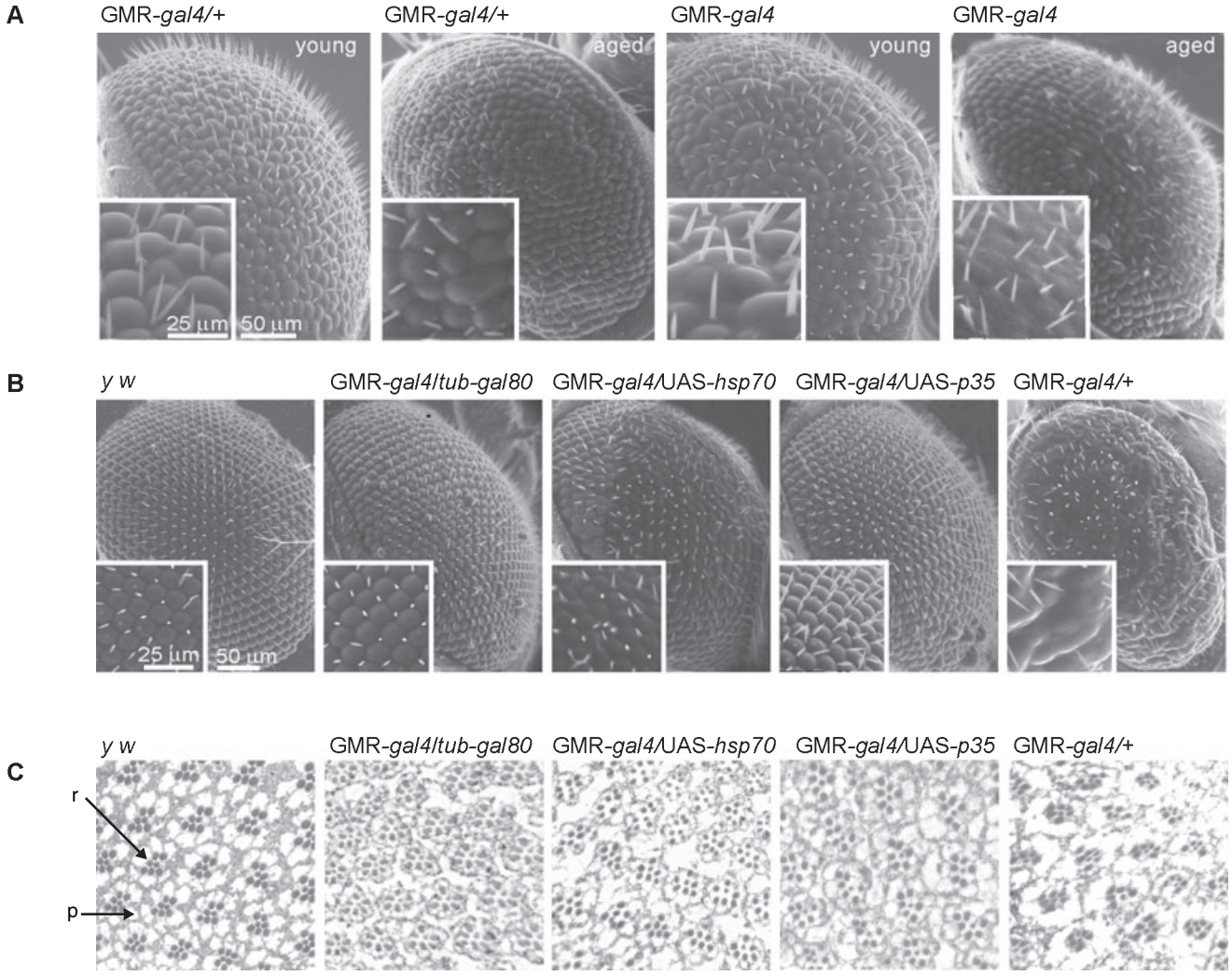

FIG. 6. Evaluation of *gal4* expression in the eye using the *glass* promoter (GMR-*gal4*). (A) Scanning electron micrographs of adult eyes from heterozygous and homozygous GMR-*gal4*. Young (0–3 days old) and aged (19–22 days old) flies maintained at 28 °C were analysed. (B) Representative images taken from *y w* and GMR-*gal4/+* aged flies expressing potential modifiers of GAL4-associated defects are shown. Insets show magnified views of relevant areas. (C) One-micrometre-thick tangential sections through the eyes of aged flies of the indicated genotypes stained with methylene blue. Sections were analysed at a level at which seven photoreceptor neurons (dark grey rhabdomeres, r) are visualized. The processes of the pigment cells (almost white in left-most panel of C), which surround each photoreceptor neuron in an ommatidium, are also indicated (p). Note the rough-eye phenotype resulting from *gal4* expression throughout eye development, and the partial rescue of the wild-type phenotype attributed to the modifiers.

Wild-type retinas do not appear to be grossly affected by normal ageing (as an example see *y w* in Fig. 6B). Instead, the GMR-*gal4* (an artificial construct with multiple GLASS binding sites; Freeman, 1996) showed a marked effect associated with the *gal4* dose. ESEM images of the external structures of the retinas expressing a single copy of GMR-*gal4* (in 1- to 3-day-old flies grown at 28 °C) showed disorganised ommatidia and loss of ommatidial bristles usually located next to facets showing supernumerary sensory hairs; fusion between contiguous ommatidia was also detected (Fig. 6A, inset); novel defects were not identified in aged heterozygous GMR-*gal4* flies, with the possible exception of a more distorted overall eye shape as well as changes in pigmentation (data not shown). These alterations were less pronounced when the flies were grown at 25 °C (data not shown), suggesting an activity-dependent origin for the defect (Duffy, 2002) in contrast to what was observed for the CNS-derived phenotypes (Fig. 1 and data not shown). Homozygous flies displayed increased defects culminating in a rough-eye phenotype (Fig. 6A).

Interestingly, constitutive expression of *tub-gal80* apparently rescued the eye phenotype observed with an ESEM in older GMR-*gal4/+* flies (Fig. 6B). Sections of ommatidia were analysed in a plane where seven photoreceptor cells were seen (Fig. 6C). A close inspection of these thin tissue sections indicated that ommatidia were somewhat affected by *gal4* expression in GMR-*gal4/tub-gal80* flies, particularly at the level of the surrounding tissue which is primarily composed of projections of the pigment cells, although the general integrity of the structure was well preserved.

Expression of *hsp70* or *p35*, on the other hand, partially rescued the rough-eye phenotype, although certain areas still showed signs of neurodegeneration (such as in the examples shown in Fig. 6B and C). Tissue sections confirmed the partial rescue at the level of the retinal array (Fig. 6C). *gal4* expression was accompanied by a collapse of the internal retinal structure, manifested as a loss of interstitial tissue and projections from pigment cells, which usually surround photoreceptor cells in each ommatidium; extreme examples exhibited loss of photoreceptor cells and even entire ommatidia (data not shown), all

phenotypes previously ascribed to cell death (Jackson *et al*., 1998; Warrick *et al*., 1998; Warrick *et al*., 1999; Kramer & Staveley, 2003).

Discussion

The GAL4/UAS system has extensively been employed in *Drosophila* and other model systems (Brand & Dormand, 1995; Kakidani & Ptashne, 1988; Brand & Perrimon, 1993). During the early stages of a genetic screen we noticed that a transgenic line expressing two copies of *gal4* performed poorly in a locomotor behaviour assay compared to its heterozygous control. Given the widespread application of this strategy to drive spatially restricted gene expression we were interested in determining the cause underlying this aberrant behaviour. We found that increased GAL4 levels associated with loss of PDF^+ neurons probably through apoptosis, which was more pronounced in those clusters expressing this exogenous protein from an earlier onset, and thus probably accumulating GAL4 to higher levels in time.

GAL4 associated defects were rescued to different levels by a defined set of modulators in the retina and central brain. Tissue sections through regions comprising both the retina and the CNS suggested an explanation for an otherwise potential contradiction between the two systems analysed (Supplementary material, Fig. S1). Meanwhile, GMR-directed GAL4 accumulation triggered cell death in CNS neurons (this study) as well as in the eye (in agreement with preliminary findings reported by Staveley and colleagues: Kramer & Staveley, 2003); it apparently did so through distinct mechanisms. In fact, GAL80, HSP70 and P35 all rescued GAL4-associated defects in the eye, albeit to a different degree (Fig. 6B and C). GAL80 appeared to reverse more efficiently the disorganisation observed in the retina, while the optic lobe (lamina and medulla; see Supplementary material, Fig. S1) as well as deeper brain structures (such as those evaluated with the PDF promoter in Fig. 5) were clearly disrupted. This result, along with the temperature dependence of the eye defect, would suggest a potential transcriptional effect associated with GAL4 expression through the development of the retina, which is different from what we observed in the central brain using two different promoters (GMR and *pdf*) to drive *gal4* expression. Nevertheless, the relative strength of the *tubulin* promoter compared to GMR and *pdf* would offer an alternative explanation to account for the differences in the ability of GAL80 to rescue GAL4-associated defects within both structures.

In contrast, both HSP70 and P35 completely rescued the behavioural phenotype (Figs 4 and 5) along with the optic lobe disruption, although the retina itself appeared somewhat disturbed (Fig. 6 and Supplementary material, Fig. S1). This observation pointed to an activity-independent effect of GAL4 accumulation in the central brain. Co-localization of TUNEL staining with GAL4-expressing cells indicated that cell death in CNS neurons was probably taking place through apoptotic mechanisms, further supporting our conclusions. The cell-type specificity of certain modifiers of GAL4-associated degeneration is in line with that reported by Ghosh & Feany (2004) for different models of polyglutamine diseases.

One of the common features of otherwise very different neurodegenerative diseases is the identification of protein aggregates (Bilen & Bonini, 2005), detectable as inclusion bodies in the cytoplasm, the nucleus or the extracellular milieu. To mention a few examples, nuclear inclusions are observed in neurons of transgenic model of HD mice (Davies *et al*., 1997) and in human HD brain tissue (DiFiglia *et al*., 1997) and they contain aggregated mutant poly Q protein, together with a growing list of cellular proteins that includes transcription factors and coregulators such as CREB-binding protein, chaperones, proteasome subunits and ubiquitin (Zoghbi & Orr, 2000; Ross, 2002). Similar protein aggregates (i.e. visible inclusions) are found in transgenic flies that express mutant poly Q repeat peptides (Feany & Bender, 2000; Jackson *et al*., 1998; Warrick *et al*., 1999; Fernandez-Funez *et al*., 2000; Marsh *et al*., 2000; Takeyama *et al*., 2002). Attempts to uncover protein aggregation associated with GAL4 excess were not successful until a highly sensitive technique was used to concentrate both the soluble and insoluble GAL4 in separate fractions, which in itself is not at all surprising given the limited number of GAL4-producing neurons. Overall our results would suggest that increased *gal4* dosage and ageing resulted in protein-folding defects that ultimately triggered its accumulation in the insoluble fraction. Thus, the aggregated protein itself could be responsible for the behavioural defects associated with the loss of PDF neurons. Likewise, our results would also argue that neurotoxicity could result from protein alterations taking place before the formation of large aggregates, most probably through protein intermediates. In fact, neurodegeneration with no formation of tau-dependent fibrillary tangles has been reported in the fly model of tauopathy (Wittmann *et al*., 2001). An alternative explanation to account for the partition of GAL4 to the insoluble fraction would be that over-expression of the nonfunctional GAL4 protein could overwhelm the degradation machinery, in turn leading to the formation of cytoplasmic aggresomes. This would explain the lack of detection of inclusion bodies in the small LNvs, although it would require a direct association of the aggregated protein with the cytoskeleton. However, we could not detect canonical components of these structures (such as the intermediate filament vimentin: Kopito, 2000; Bennett *et al*., 2005) in the extracts immunoprecipitated against GAL4, thus precluding a firm conclusion. Likewise, we could not detect ubiquitinated GAL4 forms, either in the immunoprecipitates or in whole-mount adult brains costained with anti-ubiquitin and PDF antibodies (unpublished results). In favour of the aggregation hypothesis we found that coexpression of HSP70 and P35 strongly reduced GAL4 accumulation in the insoluble fraction, which correlated with no behavioural phenotype in young (Fig. 4B) or aged (Fig. 4C, and data not shown) individuals.

GAL4 has recently been reported to correlate with increased apoptosis in fly eye imaginal discs (Kramer & Staveley, 2003), and to cause cardiac cell defects in a dose-dependent manner in a mammalian model of heart disease (Habets *et al*., 2003). In *Drosophila*, the GAL4/UAS system has extensively been employed to model a number of different poly Q diseases such as Huntington's (Jackson *et al*., 1998), and cerebrospinal ataxias type 1 and 3 (Warrick *et al*., 1998; Fernandez-Funez *et al*., 2000; Warrick *et al*., 2005), as well as Parkinson's (Feany & Bender, 2000) and Alzheimer's (Wittmann *et al*., 2001) diseases. Our data would suggest that a high level of GAL4 has adverse effects on cell viability, which may act as a sensitising agent when employing this strategy to model degenerative diseases in flies or mice. However, most of the GAL4-associated defects described in this study are the result of increasing *gal4* dosage (as in the PDF circuit in the *pdf-gal4*,UAS-*gal4* line) or activity (in the retina when employing GMR-*gal4* at 28 °C), which could be circumvented by employing several copies of the UAS (as opposed to increasing the dosage of the *gal4* driver) or lower temperatures to drive spatially restricted expression of the gene of interest. In any event, the possibility that cell death is triggered by a cellular component that becomes deregulated after the GAL4 insult, as opposed to GAL4 *per se*, has not been dismissed.

It has been reported that HSP70 rescues neurodegeneration associated with abnormal accumulation of toxic proteins (Warrick *et al*., 1999; Auluck *et al*., 2002). Likewise, expression of HSP70 in

the context of GAL4 overload not only rescued the behavioural defects but was also associated with a reduction in GAL4 in the insoluble fraction, probably through its chaperone activity (Fig. 4). In addition, coexpression of *hsp70* also resulted in decreased cell death (Fig. 5). At present we have no indication as to whether this effect is due to HSP70 modulating the apoptotic pathway, or whether it represents an indirect consequence of reducing GAL4 aggregation, or both.

Expression of a general caspase inhibitor such as P35 is sufficient to give rise to a functional PDF circuitry (judged by neuronal survival and complete rescue of behavioural rhythmicity). Although there have been reports of limited action of P35 on certain poly Q-associated fly models of disease (Ghosh & Feany, 2004; Jackson *et al*., 1998; Warrick *et al*., 1998), our observations are in line with those reported by Jackson and colleagues whereby loss of function of a programmed cell death pathway component suppressed neurodegeneration associated with expression of poly Q proteins (Sang *et al*., 2005), suggesting that preventing apoptotic cell death could be a viable strategy for circumventing some of the detrimental effects associated with the deposition of aggregated proteins.

Supplementary material

The following supplementary material may be found on www.blackwell-synergy.com

Fig. S1. GMR-*gal4* allows direct comparison of GAL4 detrimental effects on photoreceptor and central brain structures through GAL4 accumulation under the same regulatory region.

Acknowledgements

We wish to thank V. Gottifredi, E. Castaño, M.P. Fernández, J. Berni and A. Schinder for critical comments on the manuscript, and J. Cordero for comments on various eye phenotypes. We are also grateful to J. Hall, N. Bonini and the Bloomington Stock Center for sharing fly strains and to F. Rouyer for PDF antibodies. We are indebted to I. Farías for excellent help with semithin tissue sections, L. Montero for a detailed TUNEL protocol, M.E. Chiappe for initiating us into the dissection techniques, J.J. Fanara and members of his lab for advice on statistical analysis, and E. Castaño for advice on procedures with insoluble proteins. We are also grateful to A. Reynoso and M. Giordano (CITEFA, Argentina) for ESEM images. M.F.C. is a member of the Argentine Research Council (CONICET) and an HHMI International Scholar. C.R. is supported by a graduate fellowship from CONICET. This work was supported by a start-up grant from The PEW Charitable Foundation, a re-entry grant from Fundación Antorchas and the Howard Hughes Medical Institute International Research Program (n°55003668).

Abbreviations

ESEM, environmental scanning electron microscope; HD, Huntington's disease; HSP70, heat-shock protein 70; LNv, lateral neurons ventral; PBS, phosphate-buffered saline; PDF, pigment-dispersing factor; UAS, upstream activating sequence.

References

Arrasate, M., Mitra, S., Schweitzer, E.S., Segal, M.R. & Finkbeiner, S. (2004) Inclusion body formation reduces levels of mutant huntingtin and the risk of neuronal death. *Nature*, **431**, 805–810.

Auluck, P.K., Chan, H.Y., Trojanowski, J.Q., Lee, V.M. & Bonini, N.M. (2002) Chaperone suppression of alpha-synuclein toxicity in a Drosophila model for Parkinson's disease. *Science*, **295**, 865–868.

Auluck, P.K., Meulener, M.C. & Bonini, N.M. (2005) Mechanisms of suppression of {alpha}-synuclein neurotoxicity by geldanamycin in Drosophila. *J. Biol. Chem.*, **280**, 2873–2878.

Bennett, E.J., Bence, N.F., Jayakumar, R. & Kopito, R.R. (2005) Global impairment of the ubiquitin-proteasome system by nuclear or cytoplasmic protein aggregates precedes inclusion body formation. *Mol. Cell*, **17**, 351–365.

Bilen, J. & Bonini, N.M. (2005) Drosophila as a model for human neurodegenerative disease. *Annu. Rev. Genet.*, **39**, 153–171.

Bird, T.D., Nochlin, D., Poorkaj, P., Cherrier, M., Kaye, J., Payami, H., Peskind, E., Lampe, T.H., Nemens, E., Boyer, P.J. & Schellenberg, G.D. (1999) A clinical pathological comparison of three families with frontotemporal dementia and identical mutations in the tau gene (P301L). *Brain*, **122**, 741–756.

Bonini, N.M. (2002) Chaperoning brain degeneration. *Proc. Natl Acad. Sci. USA*, **99**, 16407–16411.

Bonini, N.M. & Fortini, M.E. (2003) Human neurodegenerative disease modeling using Drosophila. *Annu. Rev. Neurosci.*, **26**, 627–656.

Brand, A.H. & Dormand, E.L. (1995) The GAL4 system as a tool for unravelling the mysteries of the Drosophila nervous system. *Curr. Opin. Neurobiol.*, **5**, 572–578.

Brand, A.H. & Perrimon, N. (1993) Targeted gene expression as a means of altering cell fates and generating dominant phenotypes. *Development*, **118**, 401–415.

Ceriani, M.F., Hogenesch, J.B., Yanovsky, M., Panda, S., Straume, M. & Kay, S.A. (2002) Genome-wide expression analysis in Drosophila reveals genes controlling circadian behavior. *J. Neurosci.*, **22**, 9305–9319.

Chan, H.Y., Warrick, J.M., Gray-Board, Paulson, H.L. & Bonini, N.M. (2000) Mechanisms of chaperone suppression of polyglutamine disease: selectivity, synergy and modulation of protein solubility in Drosophila. *Hum. Mol. Genet.*, **9**, 2811–2820.

Davies, S.W., Turmaine, M., Cozens, B.A., DiFiglia, M., Sharp, A.H., Ross, C.A., Scherzinger, E., Wanker, E.E., Mangiarini, L. & Bates, G.P. (1997) Formation of neuronal intranuclear inclusions underlies the neurological dysfunction in mice transgenic for the HD mutation. *Cell*, **90**, 537–548.

DiFiglia, M., Sapp, E., Chase, K.O., Davies, S.W., Bates, G.P., Vonsattel, J.P. & Aronin, N. (1997) Aggregation of huntingtin in neuronal intranuclear inclusions and dystrophic neurites in brain. *Science*, **277**, 1990–1993.

Driscoll, M. & Gerstbrein, B. (2003) Dying for a cause: invertebrate genetics takes on human neurodegeneration. *Nat. Rev. Genet.*, **4**, 181–194.

Duffy, J.B. (2002) GAL4 system in Drosophila: a fly geneticist's Swiss army knife. *Genesis*, **34**, 1–15.

Feany, M.B. & Bender, W.W. (2000) A Drosophila model of Parkinson's disease. *Nature*, **404**, 394–398.

Fernandez-Funez, P., Nino-Rosales, M.L., de Gouyon, B., She, W.C., Luchak, J.M., Martinez, P., Turiegano, E., Benito, J., Capovilla, M., Skinner, P.J., McCall, A., Canal, I., Orr, H.T., Zoghbi, H.Y. & Botas, J. (2000) Identification of genes that modify ataxin-1-induced neurodegeneration. *Nature*, **408**, 101–106.

Freeman, M. (1996) Reiterative use of the EGF receptor triggers differentiation of all cell types in the Drosophila eye. *Cell*, **87**, 651–660.

Ghosh, S. & Feany, M.B. (2004) Comparison of pathways controlling toxicity in the eye and brain in Drosophila models of human neurodegenerative diseases. *Hum. Mol. Genet.*, **13**, 2011–2018.

Greeve, I., Kretzschmar, D., Tschape, J.A., Beyn, A., Brellinger, C., Schweizer, M., Nitsch, R.M. & Reifegerste, R. (2004) Age-dependent neurodegeneration and Alzheimer-amyloid plaque formation in transgenic Drosophila. *J. Neurosci.*, **24**, 3899–3906.

Habets, P.E., Clout, D.E., Lekanne Deprez, R.H., van Roon, M.A., Moorman, A.F. & Christoffels, V.M. (2003) Cardiac expression of Gal4 causes cardiomyopathy in a dose-dependent manner. *J. Muscle Res. Cell Motil.*, **24**, 205–209.

Hardin, P.E. (2005) The circadian timekeeping system of Drosophila. *Curr. Biol.*, **15**, R714–R722.

Hay, B.A., Wolff, T. & Rubin, G.M. (1994) Expression of baculovirus P35 prevents cell death in Drosophila. *Development*, **120**, 2121–2129.

Helfrich-Forster, C. (1997) Development of pigment-dispersing hormone-immunoreactive neurons in the nervous system of Drosophila melanogaster. *J. Comp. Neurol.*, **380**, 335–354.

Helfrich-Forster, C. (1998) Robust circadian rhythmicity of Drosophila melanogaster requires the presence of lateral neurons: a brain-behavioral study of disconnected mutants. *J. Comp. Physiol. [a]*, **182**, 435–453.

Helfrich-Forster, C. (2003) The neuroarchitecture of the circadian clock in the brain of Drosophila melanogaster. *Microsc. Res. Tech.*, **62**, 94–102.

Jackson, G.R., Salecker, I., Dong, X., Yao, X., Arnheim, N., Faber, P.W., MacDonald, M.E. & Zipursky, S.L. (1998) Polyglutamine-expanded human huntingtin transgenes induce degeneration of Drosophila photoreceptor neurons. *Neuron*, **21**, 633–642.

Kakidani, H. & Ptashne, M. (1988) GAL4 activates gene expression in mammalian cells. *Cell*, **52**, 161–167.
Kopito, R.R. (2000) Aggresomes, inclusion bodies and protein aggregation. *Trends Cell Biol.*, **10**, 524–530.
Kramer, J.M. & Staveley, B.E. (2003) GAL4 causes developmental defects and apoptosis when expressed in the developing eye of Drosophila melanogaster. *Genet. Mol. Res.*, **2**, 43–47.
Lin, Y., Stormo, G.D. & Taghert, P.H. (2004) The neuropeptide pigment-dispersing factor coordinates pacemaker interactions in the Drosophila circadian system. *J. Neurosci.*, **24**, 7951–7957.
Ma, J. & Ptashne, M. (1987) The carboxy-terminal 30 amino acids of GAL4 are recognized by GAL80. *Cell*, **50**, 137–142.
Malpel, S., Klarsfeld, A. & Rouyer, F. (2002) Larval optic nerve and adult extra-retinal photoreceptors sequentially associate with clock neurons during Drosophila brain development. *Development*, **129**, 1443–1453.
Marsh, J.L., Walker, H., Theisen, H., Zhu, Y.Z., Fielder, T., Purcell, J. & Thompson, L.M. (2000) Expanded polyglutamine peptides alone are intrinsically cytotoxic and cause neurodegeneration in Drosophila. *Hum. Mol. Genet.*, **9**, 13–25.
Muchowski, P.J. & Wacker, J.L. (2005) Modulation of neurodegeneration by molecular chaperones. *Nat. Rev. Neurosci.*, **6**, 11–22.
Palladino, M.J., Bower, J.E., Kreber, R. & Ganetzky, B. (2003) Neural dysfunction and neurodegeneration in Drosophila Na^+/K^+ ATPase alpha subunit mutants. *J. Neurosci.*, **23**, 1276–1286.
Palladino, M.J., Hadley, T.J. & Ganetzky, B. (2002) Temperature-sensitive paralytic mutants are enriched for those causing neurodegeneration in Drosophila. *Genetics*, **161**, 1197–1208.
Park, J.H., Helfrich-Forster, C., Lee, G., Liu, L., Rosbash, M. & Hall, J.C. (2000) Differential regulation of circadian pacemaker output by separate clock genes in Drosophila. *Proc. Natl Acad. Sci. USA*, **97**, 3608–3613.
Ready, D.F., Hanson, T.E. & Benzer, S. (1976) Development of the Drosophila retina, a neurocrystalline lattice. *Dev. Biol.*, **53**, 217–240.
Renn, S.C., Park, J.H., Rosbash, M., Hall, J.C. & Taghert, P.H. (1999) A pdf neuropeptide gene mutation and ablation of PDF neurons each cause severe abnormalities of behavioral circadian rhythms in Drosophila. *Cell*, **99**, 791–802.
Ross, C.A. (2002) Polyglutamine pathogenesis: emergence of unifying mechanisms for Huntington's disease and related disorders. *Neuron*, **35**, 819–822.
Ross, C.A. & Poirier, M.A. (2004) Protein aggregation and neurodegenerative disease. *Nat. Med.*, **10** (Suppl.), S10–S17.
Ross, C.A. & Poirier, M.A. (2005) Opinion: What is the role of protein aggregation in neurodegeneration? *Nat. Rev. Mol. Cell Biol.*, **6**, 891–898.
Saleh, A., Srinivasula, S.M., Balkir, L., Robbins, P.D. & Alnemri, E.S. (2000) Negative regulation of the Apaf-1 apoptosome by Hsp70. *Nat. Cell Biol.*, **2**, 476–483.
Sang, T.K., Li, C., Liu, W., Rodriguez, A., Abrams, J.M., Zipursky, S.L. & Jackson, G.R. (2005) Inactivation of Drosophila Apaf-1 related killer suppresses formation of polyglutamine aggregates and blocks polyglutamine pathogenesis. *Hum. Mol. Genet.*, **14**, 357–372.
Skovronsky, D.M., Doms, R.W. & Lee, V.M. (1998) Detection of a novel intraneuronal pool of insoluble amyloid beta protein that accumulates with time in culture. *J. Cell Biol.*, **141**, 1031–1039.
Stanewsky, R. (2003) Genetic analysis of the circadian system in Drosophila melanogaster and mammals. *J. Neurobiol.*, **54**, 111–147.
Stoleru, D., Peng, Y., Nawathean, P. & Rosbash, M. (2005) A resetting signal between Drosophila pacemakers synchronizes morning and evening activity. *Nature*, **438**, 238–242.
Takeyama, K., Ito, S., Yamamoto, A., Tanimoto, H., Furutani, T., Kanuka, H., Miura, M., Tabata, T. & Kato, S. (2002) Androgen-dependent neurodegeneration by polyglutamine-expanded human androgen receptor in Drosophila. *Neuron*, **35**, 855–864.
Warrick, J.M., Chan, H.Y., Gray-Board, Chai, Y., Paulson, H.L. & Bonini, N.M. (1999) Suppression of polyglutamine-mediated neurodegeneration in Drosophila by the molecular chaperone HSP70. *Nat. Genet.*, **23**, 425–428.
Warrick, J.M., Morabito, L.M., Bilen, J., Gordesky-Gold, B., Faust, L.Z., Paulson, H.L. & Bonini, N.M. (2005) Ataxin-3 suppresses polyglutamine neurodegeneration in Drosophila by a ubiquitin-associated mechanism. *Mol. Cell*, **18**, 37–48.
Warrick, J.M., Paulson, H.L., Gray-Board, Bui, Q.T., Fischbeck, K.H., Pittman, R.N. & Bonini, N.M. (1998) Expanded polyglutamine protein forms nuclear inclusions and causes neural degeneration in Drosophila. *Cell*, **93**, 939–949.
Wittmann, C.W., Wszolek, M.F., Shulman, J.M., Salvaterra, P.M., Lewis, J., Hutton, M. & Feany, M.B. (2001) Tauopathy in Drosophila: neurodegeneration without neurofibrillary tangles. *Science*, **293**, 711–714.
Yenari, M.A., Liu, J., Zheng, Z., Vexler, Z.S., Lee, J.E. & Giffard, R.G. (2005) Antiapoptotic and anti-inflammatory mechanisms of heat-shock protein protection. *Ann. NY Acad. Sci.*, **1053**, 74–83.
Zoghbi, H.Y. & Orr, H.T. (2000) Glutamine repeats and neurodegeneration. *Annu. Rev. Neurosci.*, **23**, 217–247.